Multi-Objective Optimization of Solid Oxide Fuel Cell/GT Combined Heat and Power System: A comparison between Particle Swarm and Genetic Algorithms

Sadegh Safari [a], Taher Hajilounezhad [b,*], Mehdi Ali Ehyaei [c]

[a] School of the Environment and Energy, Islamic Azad University- Science and Research Branch, Tehran, Iran.

[b] Department of Mechanical & Aerospace Engineering, University of Missouri, Columbia, MO, USA

[c] Department of Mechanical Engineering, Pardis Branch, Islamic Azad University, Pardis New City, Iran

ABSTRACT

Many studies have attempted to optimize integrated Solid Oxide Fuel Cell/Gas Turbine (SOFC/GT), different and somehow conflicting results are reported employing various algorithms. In this paper, Multi-Objective Optimization (MOO) is employed to approach the optimal design of SOFC/GT. The emphasis is placed on the evaluation of the Particle Swarm Optimization (PSO) and Genetic Algorithm (GA) performance as two effective tools for handling the multi-objective non-linear optimization problems. Multi- objective optimization is carried out on the electrical efficiency and the overall output power of the system is determined. The two algorithms nearly exhibit similar performance. In terms of computational effort, however, the PSO approach is faster and more efficient. The PSO appears to achieve its ultimate parameter values in fewer generations rather than the GA algorithm under the examined conditions. By comparing these two methods, it is found that the maximum power of 410 kW is achieved employing the GA optimization method, where the efficiency is 64%, while by the PSO method, the maximum power of 419.19 kW is obtained at the efficiency of 58.9%. Besides, the results stress that PSO offers more satisfactory convergence and fidelity of the solution for the SOFC-GT MOO problems.

Keywords: Modeling; Solid oxide fuel cell; Gas turbine; Multi-Objective Optimization; Heat recovery steam generation

1. Introduction

Renewable energy production techniques have been intensively studied in recent years. Among these existing technologies, solid oxide fuel cells (SOFC) have been extensively developed. Since SOFC work at high temperatures, this provides the opportunity of hybrid concepts employment such as the combination of a SOFC and a gas turbine (GT) leading to a considerable improvement of the overall system efficiency [1]. Employing internal combustion engine or solid oxide fuel cell (SOFC) and gas turbine (GT), the gaseous fuel can be turned into heat and power. However, the combination of SOFC and GT has yielded higher performance [2-4]. This hybrid conversion

* Corresponding author:
E-mail address: thnrf@mail.missouri.edu (T. Hajilounezhad)

system will provide superior utilization of natural resources that considerably decreases harmful impacts on the environment as well as making higher profit [5-7].

Typically, integrated SOFC/GT optimization issues have various objectives which may be conflicting such as capital cost, operating cost, output power, efficiency, energy consumption, and environmental impacts. In such cases, multi-objective optimization (MOO) is one of the most promising approaches for finding various Pareto optimal solutions, to comprehend the quantitative tradeoffs between the objectives and also to acquire the optimal values of decision variables [5, 8, 9]. However, various configurations of SOFC/GT hybrid systems have been studied with respect to several design parameters [10-14]. The SOFC/GT hybrid systems are usually supplied by natural gas, which is converted by means of an internal reformer. This will dramatically reduce the system capital cost since any external fuel processing will be no longer required [15].

Nevertheless, some researches have focused on the thermodynamic modeling aspects of SOFC/GT combined system [15-18], while others focused on the optimization of these systems, proposing a variety of design alternatives. A synthesis/design optimization of a hybrid SOFC/GT power plant has been investigated by the Calinse et al. [14], where a traditional single-level method based on the genetic algorithm has been developed. A thermo-economic optimization that employs a Lagrange Multiplier Approach (LMA) has been examined by Cheddie [15]. In this study, an indirectly coupled SOFC/GT hybrid power plant was considered where sizing and operating condition were employed as the decision variables to obtain the minimum lifecycle cost of the system.

Autissier et al. [19] have performed the optimization for the design of hybrid SOFC-micro GT considering two objectives; maximizing the energy efficiency and minimizing the cost. The optimization results exhibit designs with costs ranging from 2400 $/kW for a 44% energy efficiency to 6700 $/kW for a 70% energy efficiency. Sabramanyan et al. [20] have performed multi-objective optimization for a conceptual layout of a solid oxide fuel cell-proton exchange membrane fuel cell (SOFC-PEMFC) hybrid power plant. Optimizing the design of SOFC system involves consideration of the cost and performance of a SOFC-PEMFC based on a novel algorithm for minimization of single objective optimization problems (MINSOOP).

Table 1. lists a review of the literature regarding the optimization methods and strategies for SOFC/GT hybrid systems. It offers the decision variables, parameters that have been taken into consideration, objectives and the optimization approach for hybrid applications [21].

Although different optimization methods have been applied for SOFC/GT systems, none has compared the performance of these optimization methods. This work presents two optimization algorithms based on intelligent approaches for an integrated SOFC/GT system and optimizes performance of the system in order to simultaneously maximize the power output and overall efficiency.

At first, the hybrid system has been modeled in MATLAB to assess the performance characteristics of the system and thereby the system components have been evaluated to study the efficiency of the system. Since the efficiency of the SOFC/GT hybrid system is defined by the ratio of the generated power of the system to the fuel input, it is a function of several variables. Two different optimization algorithms were employed to achieve the optimal operating conditions of the entire system. As the system is extremely nonlinear, due to the combination of two extremely nonlinear systems, artificial intelligence should be practiced to optimize the whole system's performance.

Table 1. Literature review of the optimization strategies for SOFC/GT

Decision variables	Objective	Optimization Method	Application	Reference
SOFC fuel flow, operating temperature and pressure	Overall efficiency and power, total annual cost of power production and annual CO2 emission	Pareto optimal employing EA optimizer	SOFC-GT	[8]
Fuel utilization, operating pressure of fuel cell, fuel and air flow	Capital cost, cost of electricity, CO2 emissions, Power efficiency	MINSOOP algorithm employing NLP optimizer	Integrated Hybrid System	[20]
Air and fuel flows, cell voltage, air temperature	Power efficiency	Genetic Algorithm optimizer	SOFC-GT	[22]
Geometry and Operating Conditions	Overall plant cost	Genetic Algorithm using MATLAB	SOFC-GT	[23]
Temperature, Temp ratio and heat loss	Output power and efficiency	Thermodynamic analysis	SOFC-GT	[6]
Current density, pressure and temperature	Output power, efficiency of power and cost	Genetic Algorithm using MATLAB	SOFC-GT	[2]
Current density, FU, AU factor and pressure ratio	Exergy efficiency and SUCP	Genetic Algorithm using MATLAB	SOFC-GT	[3]

Mass flow rate, temperature, number of cells, FU	Period of return and exergy efficiency	GA using MATLAB	SOFC-GT	[4]

Among various existing intelligent algorithms, Genetic Algorithm (GA) and Particle Swarm Optimization (PSO), two of the most popular approaches, were selected. Both algorithms are population-based heuristic search methods that proceed towards the optimal solution by updating generations. Also, they are assumed to obtain a solution to given objective functions by employing different methodologies while interactively comparing their implementation and the results. Both GA and PSO were implemented for optimization of the combined SOFC/GT system to yield a ready comparison so that after finding the optimum parameters of the algorithms, they can be applied to systems that are more complicated [24].

As discussed earlier, there are a variety of studies that have aimed to optimize SOFC/GT cost versus power or cost versus efficiency, while only a few of them examine these two objective functions by a MOO approach for the optimization purposes. Since not all prevailing factors have been comprehensibly studied, it is still necessary to apply MOO on SOFC/GT system. Therefore, in spite of similar researches that deliberate output power and cost or the system's efficiency and cost as the objective functions, in this paper, two particular objectives including efficiency and output power are examined.

To establish the optimization framework, first the thermodynamic model of SOFC/GT hybrid system is described. Then, the Multi-Objective Optimization (MOO) is discussed and applied to the proposed system. The MOO is presented based on the simultaneous determination of optimal performance and operation by employing two different optimization methods including "Genetic Algorithm", "Particle Swarm Optimization". The considerable achievements of the proposed MOO approaches are set of optimal points (Pareto frontier) that target to identify the SOFC/GT optimal performance and operation conditions. Undoubtedly, Pareto frontiers provide supportive information for the decision-making process which is the final objective of this work.

Eventually, the results of optimization methods are presented and compared. The results include the changes in power output and efficiency of the hybrid system over the iterations employing GA and PSO. Also, the pareto diagram for both GA and PSO approach is presented.

2. Material and Methods

2.1 System description

The schematic block diagram of the proposed SOFC-GT hybrid system is depicted in Figure. 1. The system layout is divided into two main subsystems: solid oxide fuel cell (SOFC) and gas turbine (GT). Also, the system includes other auxiliary equipment such as a heat recovery steam generator (HRSG), fuel compressor, inverter, and heat exchangers. Compressed fuel is reformed into a rich hydrogen gas in an internal reforming unit, then the gas is transported into the anode compartment of the SOFC stack. In the SOFC, reformed fuel will be converted to electricity directly and DC power will be generated by an electrochemical reaction occurring within the stack, and subsequently, the generated power will be turned to AC power by employing an inverter. A portion of this electricity is used to supply electrical power source of the fuel compressor. The compressed air is used as SOFC cathode gas, after being preheated in the heat exchanger.

Unreacted gases of the anode side and preheated compressed air of the cathode participate in the combustion reaction. Combustion products will be expanded in the gas turbine for both producing additional electrical power and generating mechanical work for running the compressor. Gas turbine exhaust flow will be recovered to preheat the compressed air as well as to provide the heat required in the HRSG for producing steam used by internal reformer.

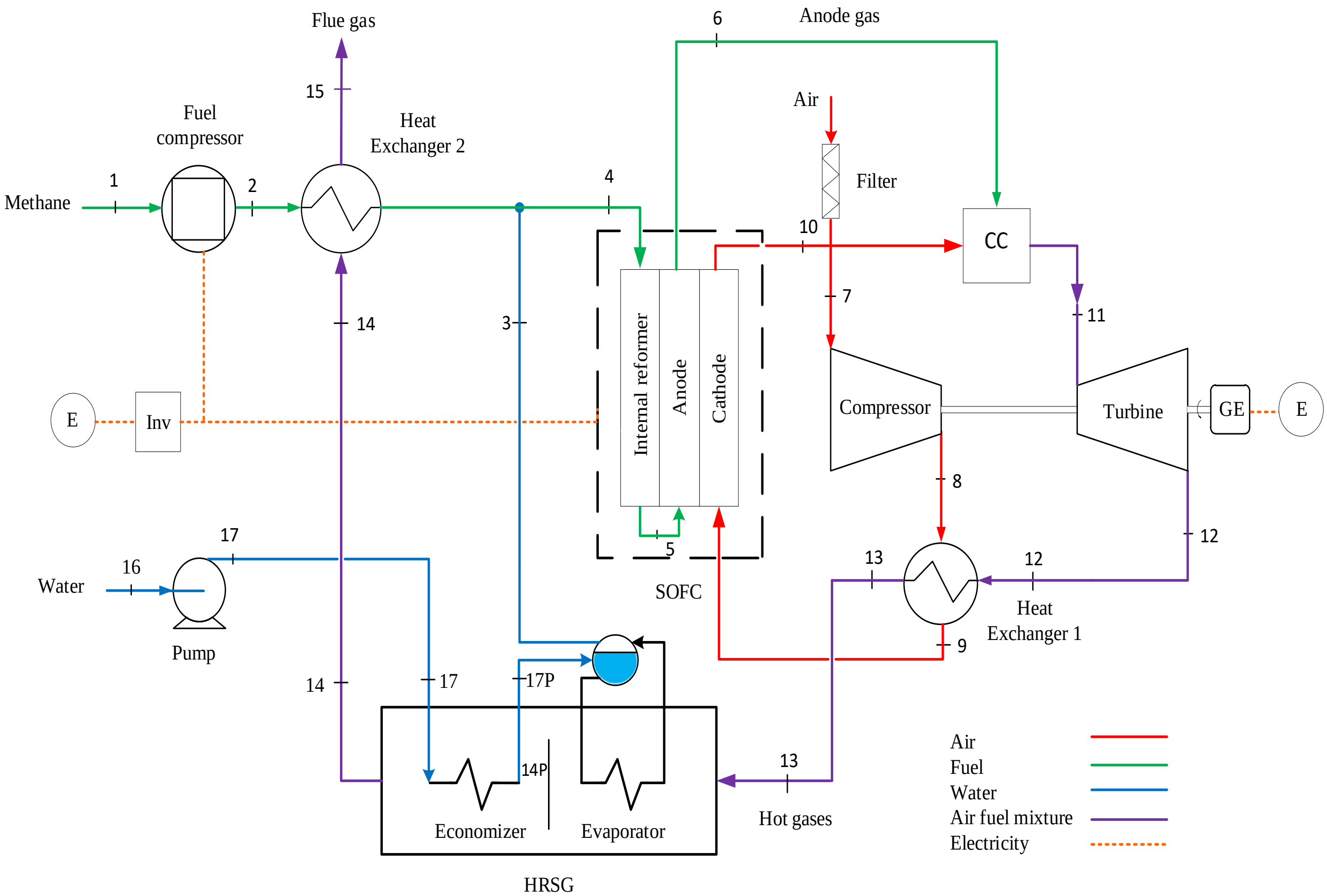

Fig. 1. The Schematic of SOFC-GT hybrid system.

2.2. Model assumptions

Principal assumptions for developing the proposed SOFC-GT hybrid system are listed as follows:

- All gases are considered as ideal gases.
- All the system components work under steady state conditions.
- The working fluid in all parts of the cycle is ideal gas.
- Internal distribution of temperature, pressure, and gas compositions in each component is uniform.
- 5% pressure drop is considered in the combustion chamber as well as fuel cell stack.
- 4% Pressure drop is assumed for heat exchanger and 5% pressure drop is assumed in the HRSG

- The inverter efficiency is assumed 0.98, the turbine mechanical efficiency is assumed 0.8 and the generator efficiency is assumed 0.97 and both air compressor and fuel compressor efficiency are assumed 0.78
- The fuel supplied to the system is assumed to be Methane.
- The dead conditions are assumed P_0=101.3 kPa and T_0= 298 K

These assumptions are employed throughout the analysis to derive the corresponding equations of each system component [25, 26].

2.3. System modeling

The model is structured based on the zero-dimensional method while mass and energy balance equations are solved simultaneously.

2.3.1. Solid oxide fuel cell

In order to optimize the SOFC-GT hybrid system parameters, it is vital to develop a SOFC model that is capable of predicting the performance based on its operating condition. The proposed SOFC is built on a tubular design which has been designed and demonstrated by Siemens-Westinghouse [27]. An electrochemical model that evaluates the power and efficiency of SOFC is developed. The geometric and material properties are selected from the literature [28].

The gas flow leaving the fuel compressor will enter the pre-reformer, then reforming and shifting reactions occur, i.e. (CH_4 + $H_2O \leftrightarrow 3H_2$ +CO) and (CO+ $H_2O \leftrightarrow H_2$+CH_4), respectively. As a result, a portion of methane will be turned into hydrogen. These reactions are considered to proceed to chemical equilibrium. The exhaust gas composition of the pre-reformer may be obtained from k_r, and k_s constants as follows [25]:

$$k_r = e^{(\Delta G_T/RT_4)} = \frac{(p_{4,H_2})^3 \cdot p_{4,CO}}{p_{4,CH_4} \cdot p_{4,H_2O}} \tag{1}$$

$$k_s = e^{(\Delta G_s/RT_4)} = \frac{p_{4,H_2} \cdot p_{4,CO_2}}{p_{4,CO} \cdot p_{4,H_2O}} \tag{2}$$

where the subscripts s and r denote the shifting and reforming reactions, respectively, R is the universal gas constant, ΔG indicates Gibbs free energy at standard conditions for the electrochemical reaction, and the partial pressures of the reacted gas streams is presented by p_i.

The fuel utilization factor, U_f, may be calculated as [25]:

$$U_f = \frac{\dot{z}}{4.\dot{m}_{4,CH_4} + \dot{m}_{4,H_2} + \dot{m}_{4,CO}} \tag{3}$$

where $\dot{z}$ indicates the hydrogen amount that reacted at the electrochemical reaction, and $\dot{m}_4$ is the mass flow rate of inlet fuel.

Maximum cell voltage is determined from the equation (4). Therefore, Nernst voltage can be formulated as follows [25]:

$$V_{nernst} = -\frac{\Delta G^0}{2F} + \frac{RT}{2F} \text{ Ln} \left[\frac{p_{H_2}.p_{o_2}{}^{1/2}}{p_{H_20}}\right] \tag{4}$$

where F refers to Faraday's constant (96485.33 $C\ mol^{-1}$), cell temperature is introduced by T and p indicates the partial pressure of respective species.

The operating voltage drops when the electric current is drawn from the cell, mainly due to some loss such as ohmic, activation and concentration polarization, which are individually categorized as electrochemical reaction activation, V_{act} ohmic polarization, V_{ohm} and concentration depletion, V_{Con}. Operating cell voltage, V_{Cell}, can be calculated as [25]:

$$V_{cell} = V_{nernst} - (V_{act} + V_{ohm} + V_{con}) \tag{5}$$

Activation polarization is calculated by the Butler-Volmer equation, expressed as [25]:

$$j = j_0 \left[\exp\left(\frac{\beta n_e F V_{act}}{RT}\right) - \exp\left(-(1-\beta)\left(\frac{n_e F V_{act}}{RT}\right)\right)\right] \tag{6}$$

where j indicates the current density, β is the transfer coefficient, and j_0 refers to exchange current density.

Ohmic polarization results from the electron and ion transmission processes is determined by the following equations based on ohm's law [28]:

$$V_{Ohm} = i\sum_k r_k \tag{7}$$

$$r_k = \sum_k \frac{\rho_k \delta_k}{A} \tag{8}$$

$$\rho_k = \sum_k a_k \exp^{\left(b_k/T\right)} \tag{9}$$

where r_k is ohmic resistance, δ_k refers to the current flow length and ρ_k indicates the material resistivity. The coefficients of a and b are the characteristics of component materials

The concentration loss which is a result of the transport of gases to the electrodes will be calculated as [28]:

$$V_{con} = \frac{RT}{2F} \, Ln \left(1 + \frac{p_{H_2}.j}{p_{H_2}.j_{lim}}\right) - \frac{R.T}{2F} Ln \left(1 - \frac{j}{j_l}\right) \tag{10}$$

where j_l is the limiting current density and j refers to the current density that will be estimated by the following electrochemical reaction [28]:

$$j = \frac{n_e.F.\dot{z}}{A_c} \tag{11}$$

where n_e is the number of electrons that are produced per hydrogen mole by electro-chemical reactions, i.e. ($H_2 + \frac{1}{2} O_2 \rightarrow H_2O$), A_c is the cell activation area and z refers to the number of hydrogen moles per second, which reacts in the electrochemical reaction. More details about calculation procedures of voltage, polarizations and current density may be found in [25, 28].

The electrical power generated from the SOFC can be calculated [25]:

$$\dot{W}_{SOFC} = N \, . \, V_{Cell} \, . \, j. A_C \tag{12}$$

where N indicates number of cells. The net electrical power of the SOFC can be given as [25]:

$$\dot{W}_{SOFC,net} = \dot{W}_{SOFC}. \eta_{inv} - \dot{W}_{FC} \tag{13}$$

Where, η_{inv} is the inverter efficiency which is assumed to be 0.98, and $\dot{W}_{FC}$ is the electrical power used by the fuel compressor.

Mass balance of SOFC considering input and output flows may be written as follows [29]:

$$\sum \dot{m}_i = \sum \dot{m}_e \tag{14}$$

$$\dot{m}_9 + \dot{m}_4 = \dot{m}_{10} + \dot{m}_6 = \dot{m}_9 + (\dot{m}_4 U_f) + \dot{m}_4(1 - U_f) \tag{15}$$

where $\dot{m}_4$ is the fuel mass rate injected to the SOFC and $\dot{m}_9$ is the air mass rate injected to SOFC. Alternatively, applying the first law of thermodynamic equation (15) can be rewritten [29]:

$$\dot{m}_9 h_9 + (\dot{m}_4 U_f) LHV + \dot{m}_4(1 - U_f) h_4 - \dot{W}_{Fc} - \dot{m}_{10} h_{10} - \dot{m}_6 h_6 = 0 \tag{16}$$

where LHV stands for the lower heating value of methane that is about 50,000 ($^{kJ}/_{kg}$). It is noteworthy that all products are considered to be adiabatic.

The energy balance for the proposed hybrid system can be written [29]:

$$\dot{m}_1 h_1 + \dot{m}_3 h_3 + \dot{m}_4 U_f LHV + \dot{Q}_{CC} - \dot{m}_{15} h_{15} - \dot{Q}_{Loss} - \dot{W}_{Fc} - \dot{W}_P - \dot{W}_{GT} = 0 \quad (17)$$

where $\dot{Q}_{CC}$ is the generated heat in combustion chamber, $\dot{Q}_{Loss}$ is the heat losses of the hybrid cycle, $\dot{W}_{Fc}$ and $\dot{W}_P$ are power used by the fuel compressor and pump, respectively and $\dot{W}_{GT}$is the output power generated by gas turbine.

2.3.2. Air compressor

The gas turbine model is comprised of the combined gas turbine and compressor with an interconnecting shaft. The irreversibility effect of the compressor is usually defined by isentropic efficiency. Accordingly, the outlet characteristics $(T_8, \bar{h}_8)$ of the air compressor can be determined from isentropic efficiency, η_{AC} and $\dot{W}_C$, the used power in the air compressor and as follows [25]:

$$\eta_{AC} = \frac{W_S}{W_a} = \frac{\bar{h}_{8s} - \bar{h}_7}{\bar{h}_8 - \bar{h}_7} \quad (18)$$

$$\frac{T_{8S}}{T_7} = \left(\frac{P_8}{P_7}\right)^{\gamma - 1/\gamma} \quad (19)$$

$$\dot{W}_{AC} = \dot{m}_7 \left(\bar{h}_8 - \bar{h}_7\right) \quad (20)$$

where T is temperature, P is pressure, h is specific enthalpy, $\dot{m}$ is mass flow rate ($^{kg}/_{S}$), η_{AC} is the air compressor efficiency and $\bar{h}_{8s}$ is the specific enthalpy of air.

2.3.3. Gas turbine

Then, the gas turbine outlet can be determined by considering the turbine isentropic efficiency, η_{tis} and expansion ratio, P_{rt} equations [25]:

$$\eta_{tis} = \frac{W_a}{W_s} - \frac{\bar{h}_{11} - \bar{h}_{12}}{\bar{h}_{11} - \bar{h}_{12s}} \quad (21)$$

$$P_{rt} = \frac{P_{11}}{P_{12}} \quad (22)$$

where $\bar{h}_{12s}$ is the specific enthalpy of fuel gas.

Further $\dot{W}_T$, the generated power by the turbine, can be determined by following equations [25]:

$$\dot{W}_T = \sum_i \left(\dot{m}_{11} \bar{h}_{11}\right)_{in} - \sum_i \left(\dot{m}_{12} \bar{h}_{12}\right)_{out} \quad (23)$$

The net power output of the gas turbine, $\dot{W}_{GT}$ can be written as:

$$\dot{W}_{GT} = \left(\dot{W}_T - \dot{W_{AC}}\right)\mu_m.\mu_g \quad (24)$$

where μ_m refers to the mechanical efficiency which is assumed 0.80 and μ_g indicates generator efficiencies which is assumed 0.98[25].

2.3.4. Combustion chamber

The exhausted fuel from the anode side of the SOFC and the off-air from the cathode side are introduced to a combustor in order to make the unreacted gases to be burnt completely for the heat recovery [29].

The combustion equation of the combustion chamber is as follows [29]:

$$\begin{aligned} & CH_4 + X_{O_2}^0 O_2 + X_{N_2}^0 N_2 + X_{CO_2}^0 CO_2 + X_{H_2O}^0 H_2O \\ & \qquad \rightarrow \left(f + X_{CO_2}^0\right)CO_2 + \left(2f + X_{H_2O}^0\right)H_2O + \left(X_{O_2}^0 - 2f\right)O_2 + X_{N_2}^0 N_2 \end{aligned} \quad (25)$$

Where, f is the molar ratio of fuel to air.

Also, the energy balance of the combustor is expressed as [29]:

$$\sum_{i=1}^{6} m_i^{in}\left(\Delta H_f^0 + \int_{298}^{T_{in}} C_p dT\right) = \sum_{i=1}^{4} m_i^{out}\left(\Delta H_f^0 + \int_{298}^{T_{out}} C_p dT\right) \quad (26)$$

Later, the adiabatic combustion temperature may be calculated by equation 26.

2.3.5. Heat recovery steam generator (HRSG)

The HRSG is used to recover energy from turbine exhausts' gas as well as generating some auxiliary steam to be utilized in an internal reformer where water is pumped to the HRSG. The steam flow rate generated by the HRSG, $\dot{m}_s$, can be calculated by considering the following equations simultaneously [30]:

$$\dot{m}_g = \dot{m}_a + \dot{m}_f \quad (27)$$

$$\dot{m}_s(h_3 - h_8) = \dot{m}_g(h_{13} - h_{14}) \quad (28)$$

$$\dot{m}_s(h_3 - h_{17P}) = \dot{m}_g(h_{13} - h_{14P}) \quad (29)$$

$$P_0 = P_{13}(1 - \Delta P_{HRSG}) \quad (30)$$

where s represents to steam and g implies gas.

2.3.6. Heat exchangers

The isentropic efficiency of the air preheater can be defined as follows [29]:

$$\varepsilon_{APH1} = \frac{T_{13} - T_8}{T_{12} - T_8} \tag{31}$$

$$\varepsilon_{APH2} = \frac{T_4 - T_2}{T_{14} - T_2} \tag{32}$$

The energy conservation equation for the air preheater can be written as [29]:

$$\dot{m}_8(h_{13} - h_8) = \dot{m}_{12}(h_{12} - h_{13})\varepsilon_{APH1} \tag{33}$$

$$\dot{m}_2(h_4 - h_2) = \dot{m}_{14}(h_{14} - h_4)\varepsilon_{APH2} \tag{34}$$

where, ε_{APH} is the isentropic efficiency of air preheater.

2.3.7. Fuel compressor

The isentropic efficiency and work of the fuel compressor can be defined as follows [26]:

$$\eta_{FC} = \frac{W_S}{W_a} = \frac{\bar{h}_{2s} - \bar{h}_1}{\bar{h}_2 - \bar{h}_1} \tag{35}$$

$$\dot{W}_{FC} = \dot{m}_f\left(\bar{h}_2 - \bar{h}_1\right) \tag{36}$$

Where $\boldsymbol{\eta_{FC}}$refers to the mechanical efficiency of fuel compressor which is assumed 0. 780.

2.3.8. Water pump

The isentropic efficiency and work of the water pump can be calculated as [26]:

$$\eta_{wp} = \frac{\bar{h}_{17s} - \bar{h}_{16}}{\bar{h}_{17} - \bar{h}_{16}} \tag{37}$$

$$\dot{W}_{WP} = \dot{m}_W\left(\bar{h}_{17} - \bar{h}_{16}\right) \tag{38}$$

2.3.9. Power and efficiency

The total energy efficiency and net power output of the proposed hybrid system including the SOFC and GT hybrid cycle is determined as following [29]:

$$\dot{W}_{net} = (\dot{W}_{SOFC} + \dot{W}_{GT} - \dot{W}_{FC} - \dot{W}_{WP}) \tag{39}$$

$$\dot{Q}_{tot} = (\dot{m}_f . U_f . LHV) \tag{40}$$

$$\eta_{HS} = \frac{\dot{W}_{net}}{\dot{Q}_{tot}} \tag{41}$$

2.4 Simulation and validation

The proposed model developed in the preceding sections is employed to simulate and assess the performance of the SOFC/GT hybrid system. The model inlet parameters for simulation of SOFC/GT system may be found in [25, 28].

In Table 2., in order to indicate the model validation and accuracy, some simulation results of the proposed model of the SOFC/GT are compared to existing studies [28]. Our results are in a reasonable agreement with counterparts in literature.

Table 2. Comparison of some simulation results of SOFC/GT system model with literature.

Parameter	Siemens-Westinghouse	Simulation results	Relative error (%)
Cell voltage (V)	0.610	0.607	-0.49
SOFC DC electrical power (kW)	187	187.53	0.28
SOFC AC electrical power (kW)	176	175.2	-0.45
GT-electrical power (kW)	47	43.04	-8.42
Net electrical power output (kW)	220	213.8	-2.81
Fist law Efficiency (%)	57	58.47	2.57

3. Optimization methods

To obtain the optimum solution for both maximum efficiency and output power of the SOFC-GT system, a mathematical method is required. There are two types of optimization methods [31]. The first category is the conventional optimization methods, like the linear programming (LP). The next one is the heuristic method. Since finding the optimum solution for the SOFC-GT hybrid system is settled in nonlinear categories and determining the optimal values with conventional methods is slightly complicated, the heuristic method has implemented in this study. Both Genetic Algorithm (GA) and Particle Swarm Optimization (PSO) are considered and employed in this optimization problems. Since both optimization approaches that have applied in this research are supposed to determine optimal solutions to a given objective function while employing different procedures, it is essential and helpful to compare their performance.

3.1. Multi-objective optimization

Recently, multi-objective optimization problems have been extensively studied, and various viable solutions have been found in the literature [2, 3, 5, 8, 20, 32]. Multi-objective problem appears virtually in different fields and has been widely applied in a variety of contexts such as, designing aircraft control systems, designing structures, and vehicles to dealing with pollution control and management problems [20].

A multi-objective optimization approach is capable of finding the solution to a problem that has two or more objectives simultaneously where the objectives are regularly in conflict with each other, such as the seek for maximum efficiency or maximum power generation and minimum cost at the same time [32].

Although there is not a unique correct solution to multi-objective optimization, there is a set of solutions whereas one is called the Pareto set. Therefore, decision making is required to select the best answers from the Pareto solutions.

The multi-objective optimization problem can be defined as [32]:

$$\mathrm{Min}_x f(x) = [\, f_1(x), f_2(x), f(x), \ldots,\ f_n(x)]^T \tag{42}$$

Subject to:

$$h_j(x) = 0 \quad j = 1,2,\ldots,n \tag{43}$$

$$g_i(x) \le 0 \quad i = 1,2,\ldots,m \tag{44}$$

Where, $f_i(x)$ refers to the i_{th} objective function, $h(x)$ and $g(x)$ are the equality and inequality constraints, respectively, and x indicates the vector of decision variables.

3.2 The MINSOOP algorithm

Although, there is a large variety of analytical methods to solve the multi-objective problems, they generally fall into two basic types: the preference-based and the generating methods. Preference-based methods such as goal programming are classical optimization techniques that integrate decision maker's preferences, thus distinguish the solution that meets the decision maker's preference perfectly. Generating approaches, such as the constraint method and the weighting method, have been widely developed to obtain the exact Pareto solution or an estimate of it.

A leading procedure for determining a solution is to consider minimizing one of the objectives while the rest are turned into inequality constraints with a parametric right-hand-side. The problem can be defined as:

$$\text{Minimize } Z_j \tag{45}$$

Subject to:

$$h(x, y) = 0 \tag{46}$$

$$g(x, y) \leq 0 \tag{47}$$

$$Z_k \leq L_k, \quad k = 1 \ldots, j-1, j+1, \ldots, p; \quad p \geq 2 \tag{48}$$

where Z_j refers to the selected jth objective that requires to be optimized. Solving frequently for various values of L_k selected between the upper, $Z_L(j)$ and lower bounds $Z_U(j)$ leads to Pareto set. In this study, The multi-objective optimization (MOO) and Minimization Single Objective Optimization Problem (MINSOOP) are employed to identify the optimal Pareto solutions to given objectives[20].

3.3 Genetic Algorithm (GA)

A genetic algorithm (GA) is an adaptive heuristic search algorithm, inspired by the evolutionary ideas of natural selection and genetics that is employed to seek for solving both constrained and unconstrained optimization problems and examine solutions to optimization problems [33].

The foremost merit of employing GA is its capability to explore in parallel and using a population of points, which assists it to avoid being trapped in a locally optimal solution. It is essential to use genetic operators such as crossover, mutation and selection at the search onset to achieve better and fitter solutions to end in a single solution. The advantage of using crossover is that it determines how the genetic algorithm merges two individuals to produce a crossover child for the next generation. It is worth mentioning that the mutation specifies the stochastic changes in populations necessary to produce mutation children. Also, the selection step enables selection of parents for the next generation [33]. The GA algorithm procedure is shown in Figure. 2.

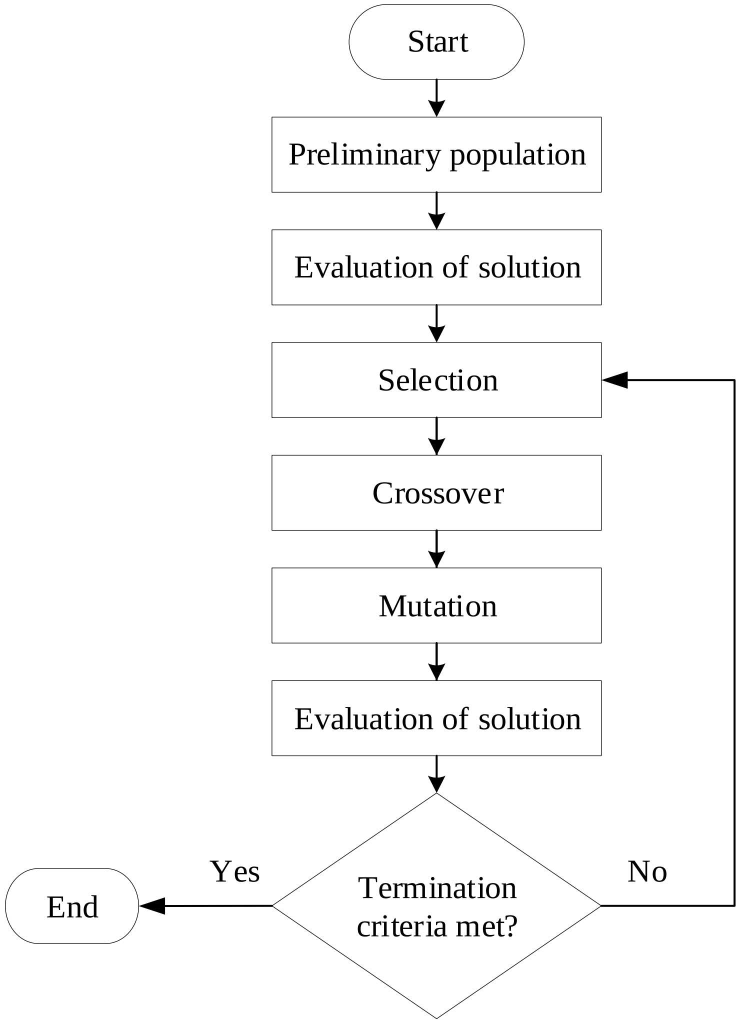

Fig. 2. the GA algorithm procedure.

As illustrated in Figure. 2, the major activity in GA is defining the fitness function that in turn reveals the solution. Then, genetic algorithm searches for a probabilistic technique to accomplish the final objective function values.

3.4. Particle Swarm Optimization (PSO)

The PSO optimization method is built on the movement and intelligence of swarms. Indeed, it is created based on how fish and birds move seeking for food. Any particle demonstrates a possible answer to a problem. The aim of the particles in the PSO is to find a global optimum point in a search space [33].

The PSO model is employed while considering the fitness value. However, the particles exhibit the fitness value solutions. Also, other features like the velocity of each particle were considered to determine the direction of particle movement. Interestingly, the particles adjust their directions corresponding to the best fitness value. It is worth noting that position and velocity are key features of every member in PSO. In this work, the collective location of the swarm and the best individual location of particles per time step are calculated. The new search orientation consists of these two orientations as well as the previous orientation [33]. Here, the best location of an individual particle and all particles for a D dimension search space may be found by equations (49) and (50), respectively.

The PSO algorithm is described as below [33]:

$$\vec{P}_1 = C_1(\vec{P}_{i1}, \vec{P}_{i2}, \dots, \vec{P}_{iD}) \tag{49}$$

$$\vec{g} = C_2(g_1, g_2, \dots, g_D) \tag{50}$$

Also, the best location in the vicinity of each particle is given by the following equation [33]:

$$\vec{n} = (n_{i1}, n_{i2}, \dots, n_{iD}) \tag{51}$$

Displacement of particles after determination their velocity is [33]:

$$\vec{X}(t) = \vec{X}(t-1) + \vec{V}(t) \tag{52}$$

$$\vec{V}(t) = \vec{V}(t-1) + \vec{F}(t-1) \tag{53}$$

The force entered in the particle can be examined by [33]:

$$\vec{F}_{i-1} = C_1(\vec{P}_{i-1} - \vec{X}_{i-1}) + C_2(\vec{g}_{i-1} - \vec{X}_{i-1}) \tag{54}$$

Here, C_1 (cognitive parameter) and C_2 (social parameter) are acceleration coefficients.

The final relation of particle velocity at dimension d and the next repetition can be written as follows [33]:

$$\begin{aligned} V_{id}(t) = \omega V_{id}(t-1) &+ C_1 r_1(\vec{P}_{id}(t-1) - \vec{X}_{id}(t-1)) \\ &+ C_2 r_2(n_{id}(t-1) - X_{id}(t-1)) \end{aligned} \tag{55}$$

This relation represents the particle velocity i at the global best. Random numbers r_1 and r_2 have a constant distribution in the range [0, 1] and ω is the inertia weight. Since it is the deterministic parameter in search behavior of swarms, hence it plays an important role in the PSO convergence quality and speed. In order to accelerate the convergence at the local optima, the parameter "X" is employed while it should be noted that it may have adverse effect and prevents convergence when excessive values are assigned to it. In practice, a value of one is assigned to "X" throughout learning and gradually and linearly reduced down to zero. An illustrative schematic of PSO algorithm is displayed in Figure 3 [33].

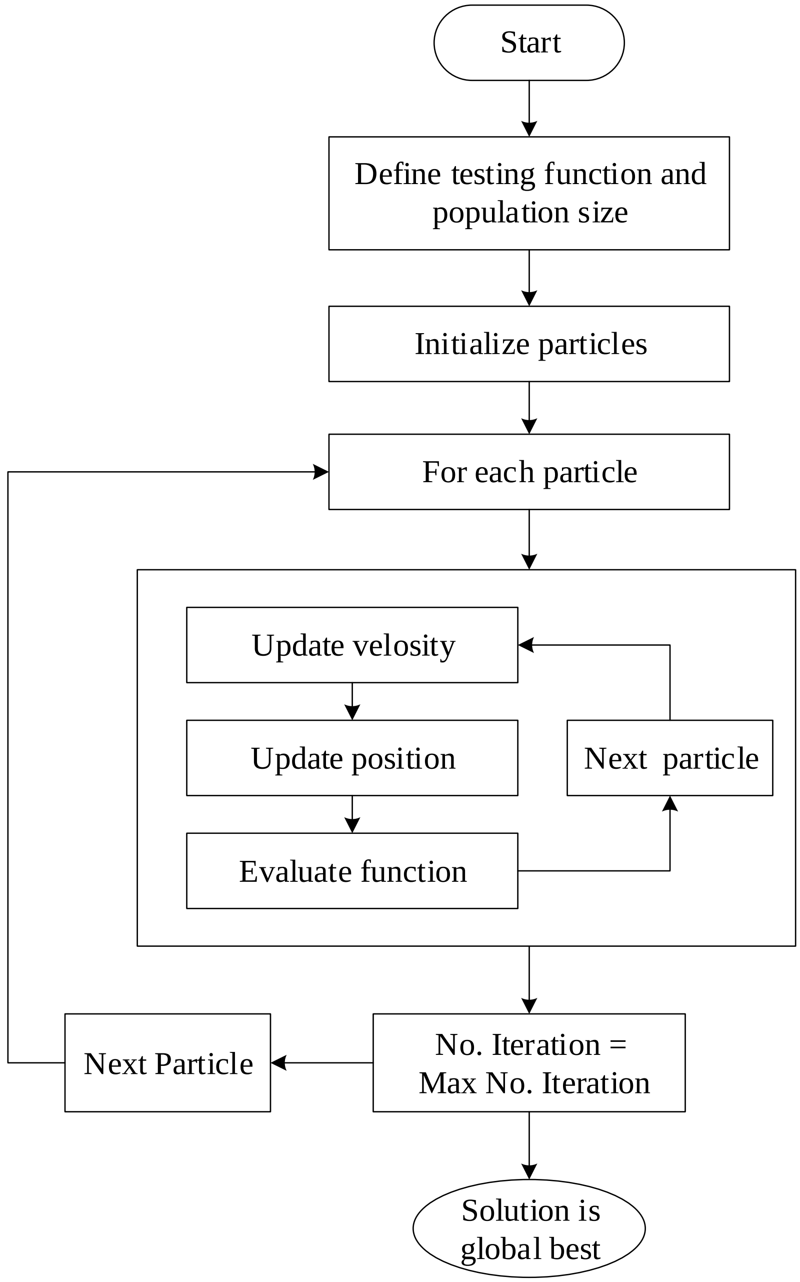

Fig. 3. PSO algorithm procedure

3.5 Objective function formulation

As discussed earlier, this work aims to investigate the optimum operating condition of the SOFC-GT system in terms of maximizing both efficiency and output power simultaneously.

Typically, the efficiency of the SOFC/GT system decreases significantly as its power output increases. Therefore, the objectives in such problems are in conflict with each other. Hence, MINSOOP approach is employed to form the objective function as follows:

$$\mathrm{Min}\ \eta_{HS}\left(U_f\, , rp_{gt}, \dot{m}_{fuel}, r_{sc}\right) = (-1)\,\frac{(\dot{W}_{SOFC} + \dot{W}_{GT} - \dot{W}_{FC} - \dot{W}_{WP})}{\dot{m}_{fuel} * U_f * LHV} \tag{56}$$

$$\mathrm{Min}\ \dot{W}_{net}\left(U_f\, , rp_{gt}, \dot{m}_{fuel}, r_{sc}\right) = (-1)(\dot{W}_{SOFC} + \dot{W}_{GT} - \dot{W}_{FC} - \dot{W}_{WP}) \tag{57}$$

where η_{HS} and $\dot{W}_{net}$ are hybrid system efficiency and the net output power, respectively, U_f is fuel utilization factor, p_{rc} refers to the pressure ratio, $\dot{m}_{fuel}$ is the mass flow rate of fuel at the anode inlet and r_{sc} is the steam to carbon ratio in the internal reformer.

It is worth noting that η_{HS} and $\dot{W}_{net}$ are the objective functions aimed to be maximized. The fitness function is formulated as follows:

$$Z = -w * \eta_{HS} - (1 - w)\dot{W}_{net} \tag{58}$$

To solve the multi-objective problems, the first step is to build a payoff table. A payoff table comprises single optimization problems, with assigned weight factors of 0 or 1 in order to find the possible ranges of the objectives $Z_U(j)$ indicates values of the upper bound, and, $Z_L(j)$ lower bound) [20].

The contrast in the scales of the parameters of these objective functions is the principal concern of optimization. The values of $\dot{W}_{tot}$ range from 42.15 kW to 408 kW. On the other hand, the values of η_{HS} lies between 0.15 and 0.88 so if the problem has solved without manipulating these conditions, the outcomes will always seek the maximum power ignoring the efficiency, regardless of the weight factor had given to the parameters [32]. To avoid this, we normalized the parameters to get the complete trade-off between 0 and 1 value [20] This approach is defined comprehensively in [34]. Finally, the fitness function is changed as:

$$Z_{Norm} = -w.\left[\frac{\eta_{HS} - 0.15}{0.88 - 0.15}\right] - (1 - w).\left[\frac{\dot{W}_{net} - 42.15}{408 - 42.15}\right] \tag{59}$$

The multi-objective optimization procedure seeks optimum values regarding the given decision variables range. However, MATLAB genetic optimization algorithm is used to achieve the optimum solutions and to model the system. PSO algorithm is also developed in MATLAB. As discussed in the previous section, the PSO algorithm principles start from an initial swarm or population and apply a research strategy based on the participation of its Ne particles.

In the PSO procedure, the speed has a pivotal role that leads the search in the promising zones of the solution area. To avoid consuming a lot of computation time, the parameter should be selected within an appropriate boundary. Population size is associated to the search space. If this parameter is too small, the algorithm is prone to converge to a local optimum; however, if the population size is too large, it will demand high computational time. After several examinations, it is found that the best performance of PSO will be accomplished when the population size is nearly 30. This value is close to the 30–50 population size pointed out in [35].

The number of PSO swarm members is assumed 30 whose positions and velocities are randomly chosen in the searching domain. Each swarm member has four dimensions, i.e. fuel utilization, pressure ratio, steam to carbon ratio and fuel flow rate. According to the system limitations, the minimum and maximum values of the four dimensions are given in Table 4.

Table 2. The limitation of parameters.

Parameter	Minimum	Maximum	Justification
Fuel utilization (%)	0.2	0.9	SOFC commercial range
Pressure ratio (bar)	2	5	Commercial restrictions
Steam to carbon ratio (S/C) (mol)	1	4	Methane reforming to hydrogen
Fuel flow rate (kg/s)	0.3	0.8	Economy of hybrid system

The parameters used in this algorithm were chosen as C1, C2= 2 and r1, r2= [0, 1]. These are the algorithm inputs, and all the parameters related to SOFC-GT hybrid system. In order to apply these limitation parameters, particles that have a position outside of this range will be penalized with a very small-scale value of objective function. Therefore, these positions are not selected by PSO algorithm as preferred position. In order to avoid the local responses and noises in algorithm output, PSO algorithm is ran three times and the best response with optimum objective function is selected as the output. Termination criteria of this algorithm is described as:

$$\frac{g_{best}^{k} - g_{best}^{k+1}}{g_{best}^{k}} < (e = 10^{-6}) \tag{60}$$

3.6 Solution methodology

In this work, we have employed a solution methodology that leads to the optimal operation conditions and set of optimal solutions for the objective functions as shown in Figure. 4. It should be noted that both technical and optimization factors are taken into consideration as illustrated in Figure. 4, namely the technical model and multi-objective optimization model including both PSO and GA algorithms. In order to solve the technical model, decision variables and constant parameters are selected followed by modelling fuel compressor, fuel processing, SOFC, GT, HRSG, and energy balance. Later, power and efficiency as the dependent variables are passed to the MOO model as objective functions to demonstrate two distinct Pareto curves using GA and PSO as solution procedures.

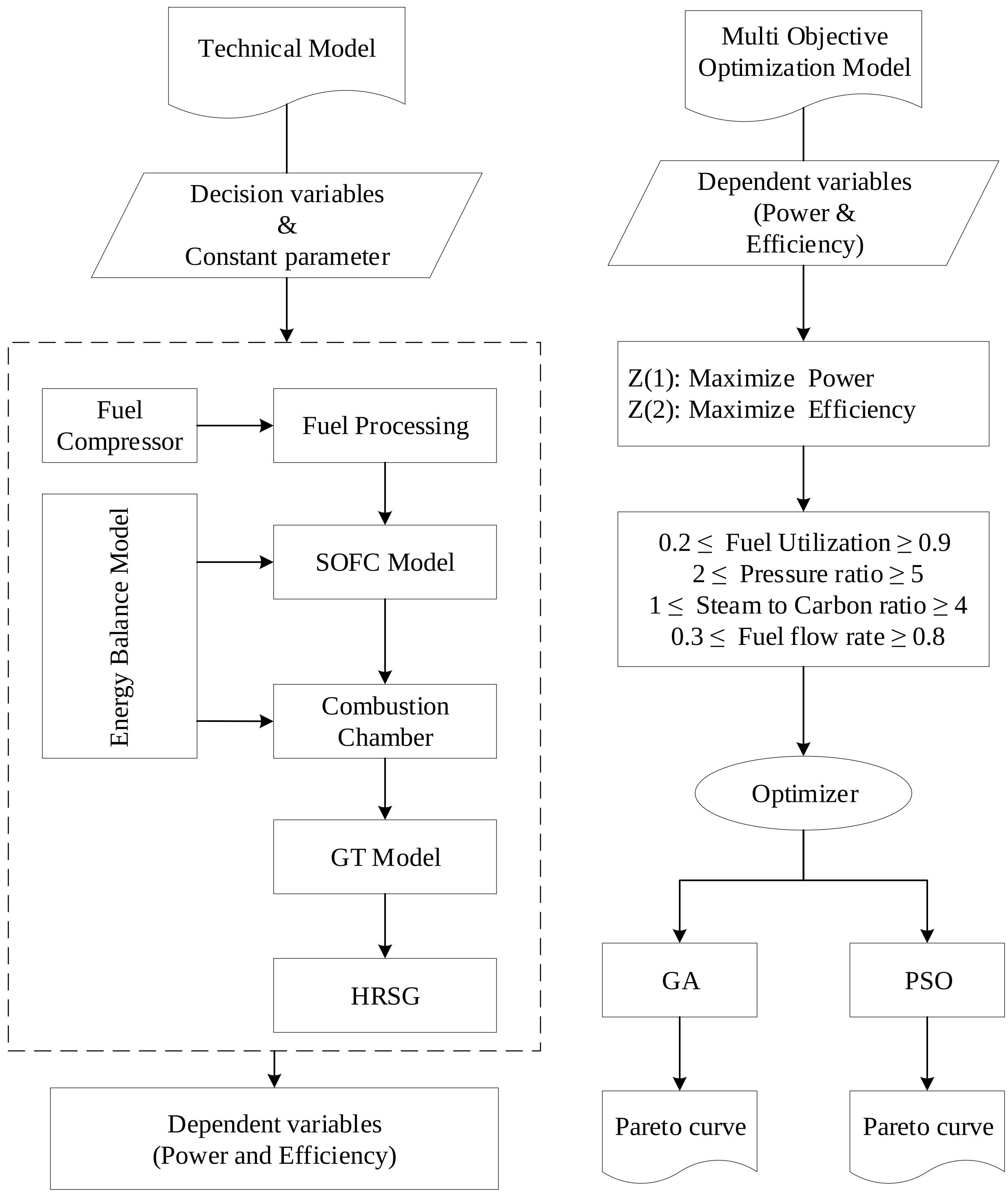

Fig. 4. Integrated SOFC/GT model solution methodology

4. Results and discussion

The results of modeling are presented first to show the impact of the operating parameters. Then, two intelligent algorithms are compared for optimizing SOFC-GT hybrid system.

4.1. Modeling results

Since the net power generation and energy efficiency of the system are the function of different parameters, the influence of some of them on SOFC-GT hybrid system is illustrated later.

The influence of the pressure ratio on SOFC/GT hybrid power system performance is illustrated in Figure. 5. The output power and efficiency of hybrid system are small at lower P_{rc} values. It is observed that increasing the pressure ratio significantly improves both the efficiency and power until it reaches some point after which pressure ratio rise only contributes to a slight enhancement. This is mainly due to the increase of the energy consumption of compressor, which consequently decreases the net power generation of gas turbine. Thus, P_{rc} range from 2 to 5 is selected and studied later, since the best improvement is experienced here, i.e. the overall power increases from 220 kW to 350 kW, also efficiency improves from 61% to 82%.

As indicated, the compressor pressure ratio has significant effect on both the net system power and efficiency as well as increasing the compressor work. It means that the compressor pressure ratio can be optimized to enhance the overall system performance.

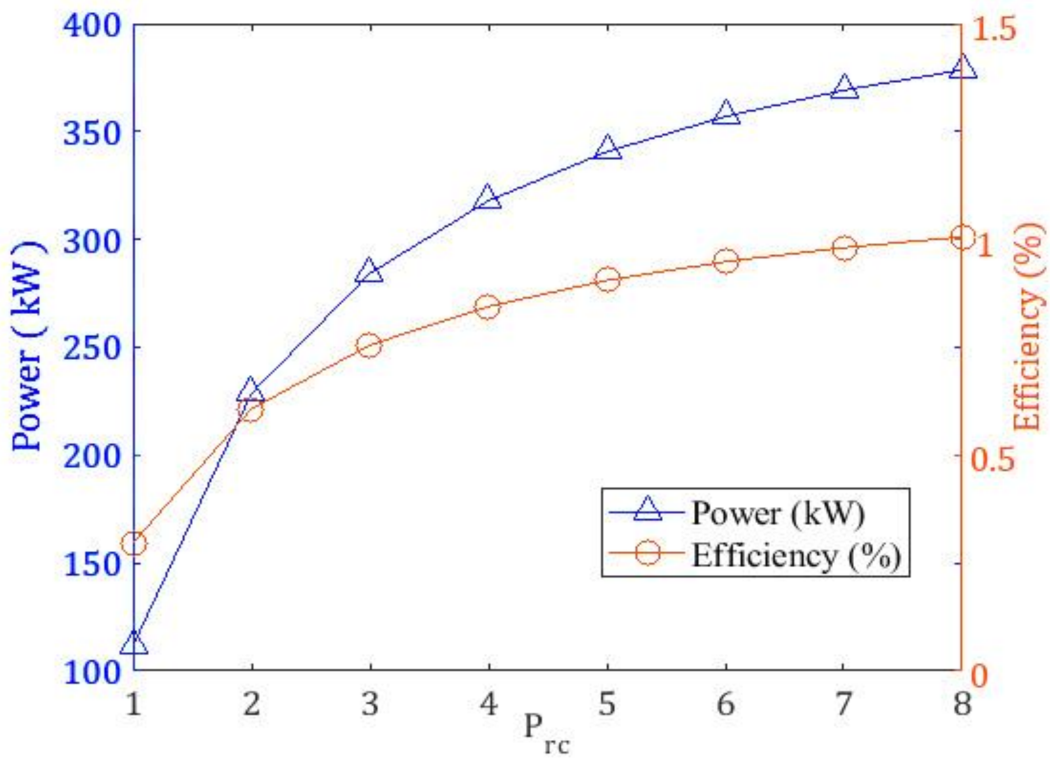

Fig. 5. The system efficiency and output power versus pressure ratio.

The fuel utilization factor U_f is an influential parameter on the power and energy efficiency of the system which signifies the ratio of hydrogen amount participated in the electrochemical reaction in the SOFC to the amount of supplied fuel.

Figure. 6 illustrates the effect of U_f on the system net output power. The power generated by the SOFC increases as U_f increases. The main reason is, while the quantity of hydrogen consumed in the SOFC increases, the operating temperature of SOFC increases as well, thus the system net output power is improved.

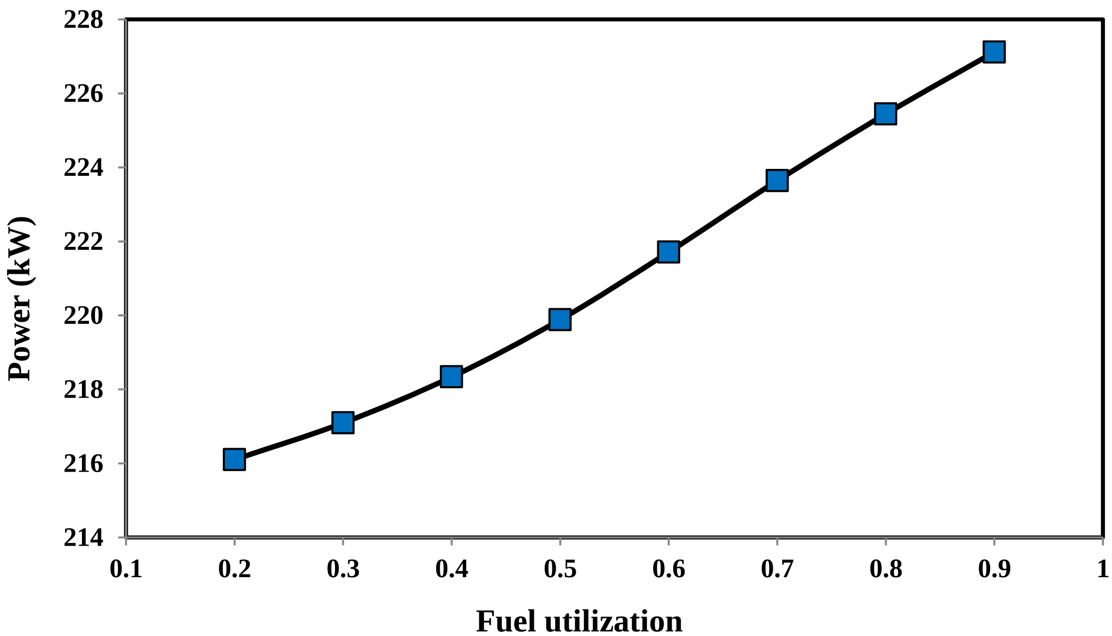

Fig. 6. Power versus fuel utilization.

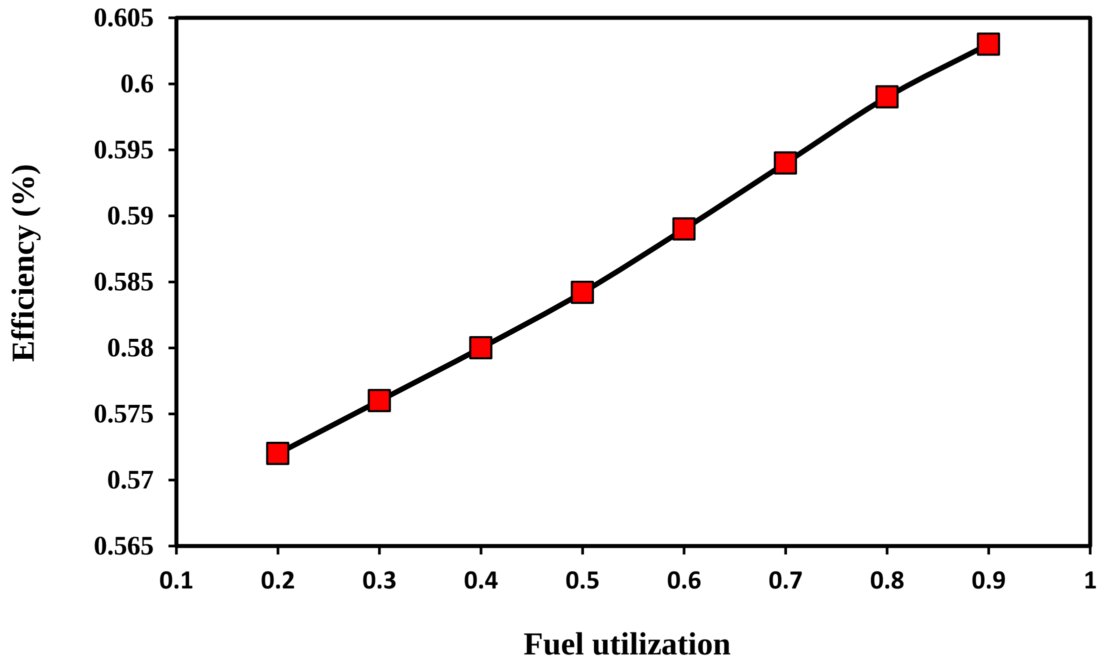

Fig. 7. Efficiency versus fuel utilization factor

The change of fuel utilization factor versus system energy efficiency is presented in Figure. 7. The efficiency enhancement trend is similar to Figure. 6, while efficiency undergoes a slightly linear improvement as fuel utilization increases. As expected, when the power increases the system energy efficiency is also improved.

Comparing Figures. 6 & 7, it is observed that at any desired condition, operating with higher fuel utilization factor leads to achieving improvement in system's power and energy efficiency. However, applying higher fuel utilization have an effect on power consumption by fuel blower. Accordingly, a tradeoff between the additional output power generation and auxiliary power consumption of blowers should be considered. Eventually, the results confirm that this an excellent choice for one of the decision variables of the system.

4.2. Optimization results

A proper comparison between the PSO and the Genetic Algorithms is performed for maximizing the net output power and the energy efficiency of the SOFC-GT system. For receiving this target, the multi-objective optimization algorithm is applied. The convergence curves of the efficiency and power versus the number of iterations are plotted in Figures 8 & 9. The same population size (P = 30) is considered in both figures.

As it is observed, the PSO algorithm has a faster convergence compared to the GA. The best output power for PSO is achieved at 432.8 s, while this happens in 620.4 s for GA. This reveals that the PSO approach reaches the optimum solution 287.6 s faster than the GA when using the same population size.

This is mainly because PSO does not possess genetic operators like mutation consequently, particles will be updated regarding the internal velocity. Due to their memory as well as unique information sharing mechanism where only the best particle reveals the information to others, the PSO excels to find the best solution more efficiently in comparison to GA. Further, PSO finds a better solution with a lower number of iterations. In this study, the best solution of power is achieved by 39 convergence iterations when employing PSO, while GA reaches the best solution in 56 convergence iterations.

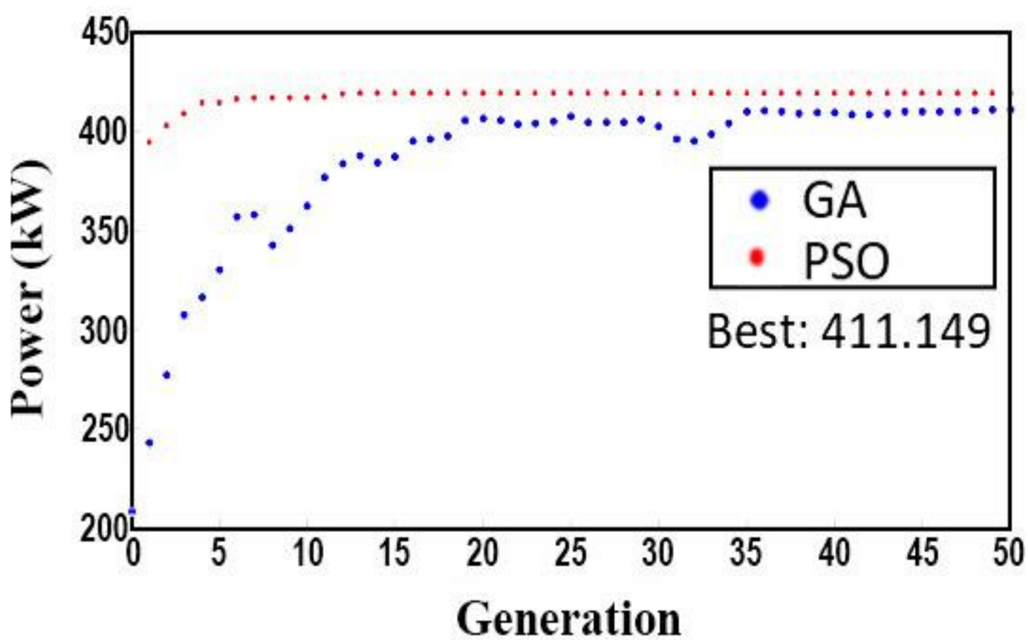

Fig. 8. The system power over generations.

As shown in Figure. 9, similar to the optimization of the system power, the PSO algorithm has better performance optimizing the efficiency. The PSO algorithm indicates faster convergence where it reaches to the best efficiency at 507.2 s in comparison to GA obtaining the best efficiency at 586.15 s. It is clear that the PSO approach reaches the optimum solution 78.95 s faster than GA.

These results are compatible with references [35, 36]. Regarding an evolutionary viewpoint, the performance of the PSO is significantly better than the GA such that PSO shows to succeed at its final parameter values in fewer generations compared to the GA. Moreover, it is observed that the PSO algorithm reaches to the best solution at approximately 20 generations for energy efficiency optimization. This is mainly since the PSO algorithm is comprised of particles that are randomly initialized and they are influenced by their best past location. The particles update themselves with the internal velocity and have memory that makes it faster than GA.

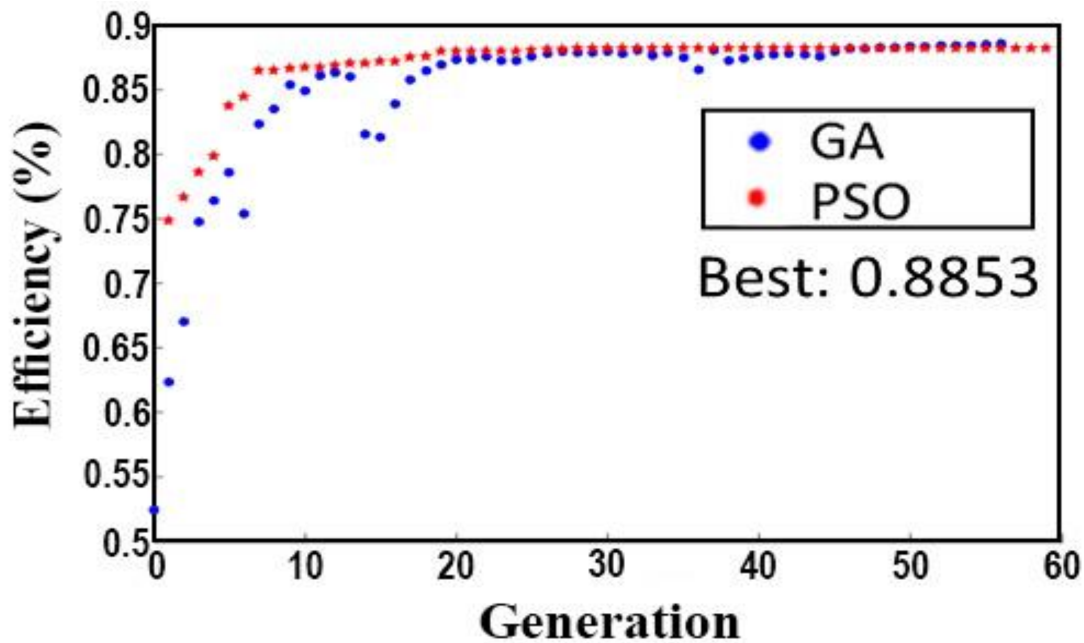

Fig. 9. The system efficiency over generations.

The output power optimization versus efficiency objective function considering the PSO and GA procedures is shown in Figures. 10&11, respectively. Pareto front diagrams are generated for the purpose of trade-off analysis between energy efficiency and the net output power. As already anticipated, the conflict between the considered objective functions is evident in Figure. 10. It may be seen that improving the power in the set leads to hindering the efficiency.

In analyzing the energy efficiency and net output power alternatives, decision makers often seek to know the optimum solution between tow objective functions. For instance, if it is aimed to generate the maximum power, i.e. 419.2 kW, the energy efficiency will be equal to 58%. In contrast, if the highest energy efficiency is targeted, i.e. 88%, the net output power will be about

210 kW. Therefore, Pareto optimality allows decision makers to choose between target functions in accordance with optimal performance requirements.

Since the diagram slope changes drastically below the energy efficiency of 74% and the net output power of 360 kW, the best optimum solution in terms of both the energy efficiency and the net output power is determined in the specified region marked in Figure. 10. It is observed from the Pareto optimality that for producing 402 kW power, the energy efficiency is equal to 67% whereas the energy efficiency improves approximately by 10 % and reaches up to 73.7% when the net output power reaches to 364kW, that is equal to 9.4% drop in power generation.

On the other hand, if the energy efficiency of 84% is intended, the power generation will be equal to 270 kW. This means if the efficiency improves by 25% the power generation will be dropped by 32.8%.

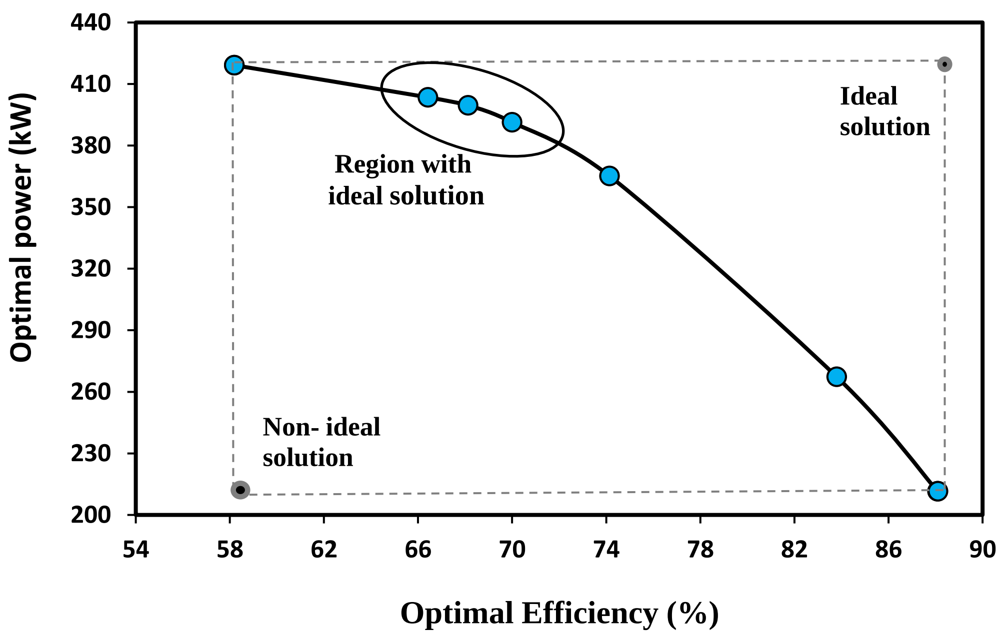

Fig. 10. The Pareto optimality diagram of PSO.

The variation in the decision variables regard to a variety of weighting factors by the GA approach is shown in Figure. 11. In the Pareto front, point A (W=0) indicates the maximum power generation, 410.5 kW, at 64% efficiency. As it is clear, by increasing the weighting factor (W) or enhancing the importance of the energy efficiency, less power is generated while the efficiency will be enhanced gradually. In the other side, point B (W=1) refers to the maximum efficiency of

88% for the 210kW power generation. Based on this trade off of the Pareto optimality, the decision makers are able to adjust the efficiency in respect to the expected power generation and vice versa. By comparing these two Pareto front diagrams, it can be seen that in the GA optimization method, the maximum net output power of 410 kW is achieved while the energy efficiency is 64%, whereas in the PSO method the maximum net output power of 419.2kW is obtained at the energy efficiency of 58.9%.

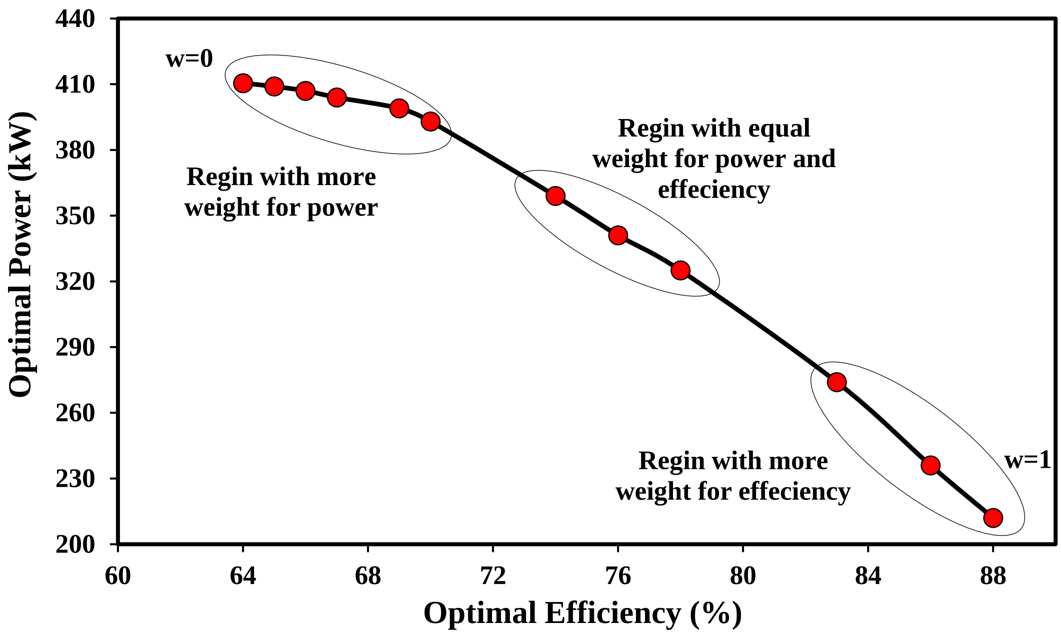

Fig. 5. The Pareto optimality diagram of GA.

To make a ready comparison, the parameters of both algorithms are summarized in Table 5.

Table 3. The algorithm parameters.

PSO coefficient	Value	GA coefficient	Value
C_1, C_2	2	**Population**	30
W_{max}	30	**Mutiation**	0.01
W_{min}	1	**Crossover**	0.8

Moreover, the best results obtained from the two proposed algorithms are compared and briefly indicated in Table 6. It can be found that the best solution achieved by the PSO method is obtained when the energy efficiency and net output power is 88.2% and 419.2 kW, respectively. Also, the GA optimization method outcomes 88 % and 410.5 kW for the energy efficiency and net output power, respectively. The PSO not only provides a better speed response compared to the GA in terms of computational results, but also yields a better energy efficiency in terms of computational time minimization.

It is observed that the effect of the fuel utilization factor on improving the energy efficiency is greater than on the net output power. The optimum net output power in the PSO method is achieved by the fuel utilization factor of 0.79 while the GA reaches to the optimum solutions by a fuel utilization of 0.85.

The fuel utilization factor is a pivotal parameter which is remarkably associated with the performance of SOFCs and reflects the performance of the hybrid systems. Higher utilization factor is reached when a larger portion of the inlet fuel reacts in SOFC, and a smaller portion is introduced into the combustion chamber of the GT. The fuel utilization factor enhancement means more fuel is involved in the electrochemical reactions, thus in the anode outlet, the percentage of CO_2 will be increased rather than H_2 and CO. Consequently, the power generation by the GT cycle will be decreased. On the other hand, as U_f is boosted, the electrochemical reaction rates rise, hence the electrical power output generated by the SOFC is improved. As expected, the participation of the SOFC to the total output power of 419 kW increases by increasing the U_f . In addition, the higher U_f utilizes a higher SOFC cell temperature, that leads to higher turbine inlet temperature, thus higher GT efficiency.

Therefore, in order to provide reasonable energy efficiency and net output power, the fuel U_f is required to be maintained between 0.79 and 0.85 according to this simulation which agrees with commercial SOFC U_f values in the market [37]. Increasing of the fuel mass flow rate will increase the current density and voltage in the SOFC that results in more power generation. In contrast, the higher fuel consumption has a negative effect on the energy efficiency. Also, steam offered the best performance as reforming agent for methane with respect to results observed from the simulation and both optimization methods.

Table 4. The results of optimized key parameters of the system

Optimization Algorithm	**PSO**	**GA**

Objective	Energy efficiency	Output power	Energy efficiency	Output power
Maximum value	88.2 %	419.2 kW	88 %	410.5 kW
Convergence iteration	47	39	51	56
Convergence time	507.2 s	432.8s	586.15 s	620.4 s
Fuel utilization	0.9	0.79	0.9	0.85
Pressure ratio	4.12	4.16	4.16	4.23
Steam to carbon ratio (S/C)	4	4	4	3.99
Fuel mass flow rate	0.3	0.9	0.3	0.8

In particular, when comparing these results to those of previous studies, it should be pointed out that the system energy efficiency achieved here is significantly higher compared to other studies [38]. This is not only due to the particular optimization procedure but also may originate from the fact that the isentropic efficiencies of the compressor and turbine in the GT cycle are considered higher than [38].

Also, the present work employs the individual layout and components such as fuel compressor and heat exchangers to increase the operating pressure and temperature of the system. Increasing the operating temperature in SOFC leads to the increase of the voltage thus improvement of the energy efficiency as well as the net output power of the system. At higher operating temperature, the system generates more power. The reason is, as a result of higher operating temperature, speed of reactions is increased and the lower voltage drop occurs in the SOFC that leads to higher production voltages, therefore, more power generation.

Besides, as temperature is increased, the less quantity of air is required to react. So, the lower air mass flow rate is entered into the system. Since the compressor power consumption is directly related to the inlet air mass flow rate, the compressor also consumes less power. The simultaneous effect of increasing the voltage and reducing the power consumption of the compressor is the enhancement of the power generation of the system. On the other hand, while the operating system pressure increases, the voltage drops. As a result, the concentration polarization will be decreased, consequently, the system net output power will be enhanced.

5. Conclusions

In this paper, in order to simultaneously enhance the energy efficiency and the net output power, a hybrid SOFC-GT system is studied by two evolutionary Multi-Objective Optimization algorithms. The optimum operating conditions of the integrated SOFC-GT system, i.e. fuel utilization factor, fuel mass flow rate, pressure ratio and steam to carbon ratio, are determined that suggests a significant performance improvement. This enhancement results from recovering the heat of the exhaust gases of SOFC followed by preheating and substituting the fuel from methane to hydrogen. Pareto curves are employed to find the desired power output at the maximum efficiency with refence to both PSO and GA approaches.

Genetic algorithm (GA) and Particle Swarm Optimization (PSO) methods were compared and applied to the system. The results indicate that both the GA and the PSO can be considered in the MOO models. The two algorithms nearly exhibit similar performance. In terms of computational effort, however, the PSO approach is faster and more efficient. The PSO appears to achieve its ultimate parameter values in fewer generations rather than the GA algorithm under-examined conditions. In addition, it requires a smaller number of function evaluations compared to the GA. It should be noted that neither two mentioned algorithms take short time to obtain their results. Regarding the accuracy of the model parameters, the GA approach matches more alike to the pre-existing values. It is concluded from the current comparison that the PSO algorithm is more suitable for the SOFC-GT MOO problem than the GA.

References

[1] Y. Zhao, N. Shah, N. Brandon, Comparison between two optimization strategies for solid oxide fuel cell–gas turbine hybrid cycles, international journal of hydrogen energy 36(16) (2011) 10235-10246.
[2] R. Roshandel, A. Behzadi Forough, Two strategies for multi-objective optimisation of solid oxide fuel cell stacks, International Journal of Sustainable Energy 33(4) (2014) 854-868.
[3] L. Khani, A.S. Mehr, M. Yari, S. Mahmoudi, Multi-objective optimization of an indirectly integrated solid oxide fuel cell-gas turbine cogeneration system, International Journal of Hydrogen Energy 41(46) (2016) 21470-21488.
[4] H.A. Reyhani, M. Meratizaman, A. Ebrahimi, O. Pourali, M. Amidpour, Thermodynamic and economic optimization of SOFC-GT and its cogeneration opportunities using generated syngas from heavy fuel oil gasification, Energy 107 (2016) 141-164.
[5] S. Sharma, F. Maréchal, Robust Multi-Objective Optimization of Solid Oxide Fuel Cell–Gas Turbine Hybrid Cycle and Uncertainty Analysis, Journal of Electrochemical Energy Conversion and Storage 15(4) (2018) 041007-041007-9.
[6] Y. Zhao, N. Shah, N. Brandon, The Development and Application of a Novel Optimisation Strategy for Solid Oxide Fuel Cell-Gas Turbine Hybrid Cycles, Fuel Cells 10(1) (2010) 181-193.
[7] J. Brown, T. Hajilounezhad, N.T. Dee, S. Kim, A.J. Hart, M.R. Maschmann, Delamination Mechanics of Carbon Nanotube Micropillars, ACS Applied Materials & Interfaces 11(38) (2019) 35221-35227.
[8] M. Burer, K. Tanaka, D. Favrat, K. Yamada, Multi-criteria optimization of a district cogeneration plant integrating a solid oxide fuel cell–gas turbine combined cycle, heat pumps and chillers, Energy 28(6) (2003) 497-518.

[9] F. Mobadersani, H. Safari, T. Hajilounezhad, P. Kahroba, The Effect of Fluid Properties on the Operation of Thermal Bubble jet, arXiv preprint arXiv:1910.07901 (2019).
[10] X. Zhang, S. Chan, G. Li, H. Ho, J. Li, Z. Feng, A review of integration strategies for solid oxide fuel cells, Journal of Power Sources 195(3) (2010) 685-702.
[11] W. Burbank Jr, D. Witmer, F. Holcomb, Model of a novel pressurized solid oxide fuel cell gas turbine hybrid engine, Journal of Power Sources 193(2) (2009) 656-664.
[12] T. Hajilounezhad, D.M. Ajiboye, M.R. Maschmann, Evaluating the Forces Generated During Carbon Nanotube Forest Growth and Self-Assembly, Materialia (2019) 100371.
[13] T. Gengo, Y. Ando, T. Kabata, Development of 200 kW class SOFC combined cycle system and future view, Technical Review. Mitsubishi Heavy Industries, Ltd 45 (2008).
[14] T. Hajilounezhad, Z.A. Oraibi, R. Surya, F. Bunyak, M.R. Maschmann, P. Calyam, K. Palaniappan, Exploration of Carbon Nanotube Forest Synthesis-Structure Relationships Using Physics-Based Simulation and Machine Learning.
[15] A. Buonomano, F. Calise, M.D. d’Accadia, A. Palombo, M. Vicidomini, Hybrid solid oxide fuel cells–gas turbine systems for combined heat and power: a review, Applied Energy 156 (2015) 32-85.
[16] F. Calise, A. Palombo, L. Vanoli, Design and partial load exergy analysis of hybrid SOFC–GT power plant, Journal of power sources 158(1) (2006) 225-244.
[17] T. Hajilounezhad, M.R. Maschmann, Numerical Investigation of Internal Forces During Carbon Nanotube Forest Self-Assembly, ASME 2018 International Mechanical Engineering Congress and Exposition, American Society of Mechanical Engineers, 2018, pp. V002T02A088-V002T02A088.
[18] W. Lundberg, S. Veyo, M. Moeckel, A high-efficiency solid oxide fuel cell hybrid power system using the Mercury 50 advanced turbine systems gas turbine, Journal of Engineering for Gas Turbines and Power 125(1) (2003) 51-58.
[19] N. Autissier, F. Palazzi, F. Maréchal, J. Van Herle, D. Favrat, Thermo-economic optimization of a solid oxide fuel cell, gas turbine hybrid system, Journal of fuel cell science and technology 4(2) (2007) 123-129.
[20] K. Subramanyan, U.M. Diwekar, A. Goyal, Multi-objective optimization for hybrid fuel cells power system under uncertainty, Journal of power sources 132(1-2) (2004) 99-112.
[21] F. Ramadhani, M. Hussain, H. Mokhlis, S. Hajimolana, Optimization strategies for Solid Oxide Fuel Cell (SOFC) application: A literature survey, Renewable and Sustainable Energy Reviews 76 (2017) 460-484.
[22] B.F. Möller, J. Arriagada, M. Assadi, I. Potts, Optimisation of an SOFC/GT system with CO2-capture, Journal of Power Sources 131(1-2) (2004) 320-326.
[23] F. Calise, M.D. d’Accadia, L. Vanoli, M. Von Spakovsky, Single-level optimization of a hybrid SOFC–GT power plant, Journal of Power Sources 159(2) (2006) 1169-1185.
[24] A. Konak, D.W. Coit, A.E. Smith, Multi-objective optimization using genetic algorithms: A tutorial, Reliability Engineering & System Safety 91(9) (2006) 992-1007.
[25] A.V. Akkaya, B. Sahin, H.H. Erdem, An analysis of SOFC/GT CHP system based on exergetic performance criteria, International Journal of Hydrogen Energy 33(10) (2008) 2566-2577.
[26] A.B. Forough, R. Roshandel, Design and operation optimization of an internal reforming solid oxide fuel cell integrated system based on multi objective approach, Applied Thermal Engineering 114 (2017) 561-572.
[27] R.A. George, Status of tubular SOFC field unit demonstrations, Journal of Power Sources 86(1-2) (2000) 134-139.
[28] A.V. Akkaya, Electrochemical model for performance analysis of a tubular SOFC, International Journal of Energy Research 31(1) (2007) 79-98.
[29] M. Shamoushaki, M. Ehyaei, F. Ghanatir, Exergy, economic and environmental analysis and multi-objective optimization of a SOFC-GT power plant, Energy 134 (2017) 515-531.
[30] B.A. Yazdi, B.A. Yazdi, M.A. Ehyaei, A. Ahmadi, Optimization of micro combined heat and power gas turbine by genetic algorithm, Thermal Science 19(1) (2015) 207-218.
[31] F. Calise, M.D. d’Accadia, L. Vanoli, M.R. von Spakovsky, Full load synthesis/design optimization of a hybrid SOFC–GT power plant, Energy 32(4) (2007) 446-458.
[32] S.O. Mert, Z. Özçelik, Y. Özçelik, I. Dinçer, Multi-objective optimization of a vehicular PEM fuel cell system, Applied Thermal Engineering 31(13) (2011) 2171-2176.
[33] H. Sadeghzadeh, M. Ehyaei, M. Rosen, Techno-economic optimization of a shell and tube heat exchanger by genetic and particle swarm algorithms, Energy Conversion and Management 93 (2015) 84-91.
[34] R.T. Marler, J.S. Arora, Survey of multi-objective optimization methods for engineering, Structural and multidisciplinary optimization 26(6) (2004) 369-395.

[35] P.R. López, M.G. González, N.R. Reyes, F. Jurado, Optimization of biomass fuelled systems for distributed power generation using particle swarm optimization, Electric Power Systems Research 78(8) (2008) 1448-1455.
[36] S. Panda, N.P. Padhy, Comparison of particle swarm optimization and genetic algorithm for FACTS-based controller design, Applied soft computing 8(4) (2008) 1418-1427.
[37] R.J. Braun, Optimal design and operation of solid oxide fuel cell systems for small-scale stationary applications, (2002).
[38] Q. Meng, J. Han, L. Kong, H. Liu, T. Zhang, Z. Yu, Thermodynamic analysis of combined power generation system based on SOFC/GT and transcritical carbon dioxide cycle, International Journal of Hydrogen Energy 42(7) (2017) 4673-4678.